

This is the peer-reviewed, manuscript version of an article published in the *Journal of Biomechanics*.

© 2018. This manuscript version is made available under the CC-BY-NC-ND 4.0 license <http://creativecommons.org/licenses/by-nc-nd/4.0/>.

The full details of the published version of the article are as follows:

TITLE: Uncovering the structure of the mouse gait controller: mice respond to substrate perturbations with adaptations in gait on a continuum between trot and bound

AUTHORS: Vahedipour, A; Haji Maghsoudi, O; Wilshin, S; Shamble, P; Robertson, B; Spence, A

JOURNAL: Journal of Biomechanics

PUBLISHER: Elsevier

PUBLICATION DATE: 17 July 2018 (online)

DOI: [10.1016/j.jbiomech.2018.07.020](https://doi.org/10.1016/j.jbiomech.2018.07.020)

Uncovering the structure of the mouse gait controller: mice respond to substrate perturbations with adaptations in gait on a continuum between trot and bound

A. Vahedipour¹, O. Haji Maghsoudi¹, S. Wilshin², P. Shamble^{1,3}, B. Robertson^{1,4}, A. Spence¹;

¹ Department of Bioengineering, Temple University, Philadelphia, PA, 19122, USA.

² Structure and Motion Laboratory, Royal Veterinary College, University of London, London, United Kingdom.

³ *Current affiliations:* (1) John Harvard Distinguished Science Fellowship Program, Harvard University, Cambridge, MA 02138, USA. (2) Department of Organismic and Evolutionary Biology, Harvard University, Cambridge, MA 02138, USA.

⁴ Current affiliation: Edgewise Therapeutics, Boulder, CO, 80303, USA.

Corresponding Author:

Corresponding Author:

Annie Vahedipour,
PhD Candidate
Department of Bioengineering
Engineering Building Room 819
College of Engineering
Temple University
1947 N. 12th Street
Philadelphia, PA 19122
Phone: 214-546-7868
Email: annie.vahedipour@temple.edu

Article Type: Full length Article

Word count: 3495

Keywords: Gait, Perturbation, Bounding, Mice, Treadmill

Abstract

Animals, including humans, have been shown to maintain a gait during locomotion that minimizes the risk of injury and energetic cost. Despite the importance of understanding the mechanisms of gait regulation, ethical and experimental challenges have prevented full exploration of these. Here we present data on the gait response of mice to rapid, precisely timed, spatially confined mechanical perturbations. Our data elucidate that after the mechanical perturbation, the mouse gait response is anisotropic, preferring deviations away from the trot towards bounding, over those towards other gaits, such as walk or pace. We quantified this shift by projecting the observed gait onto the line between trot and bound, in the space of quadrupedal gaits. We call this projection λ . For $\lambda = 0$, the gait is the ideal trot; for $\lambda = \pm\pi$, it is the ideal bound. We found that the substrate perturbation caused a significant shift in λ towards bound during the stride in which the perturbation occurred and the following stride (linear mixed effects model: $\Delta\lambda = 0.26 \pm 0.07$ and $\Delta\lambda = 0.21 \pm 0.07$, respectively; random effect for animal, $p < 0.05$ for both strides, $n = 8$ mice). We hypothesize that this is because the bounding gait is better suited to rapid acceleration or deceleration, and an exploratory analysis of jerk showed that it was significantly correlated with λ ($p < 0.05$). Understanding how gait is controlled under perturbations can aid in diagnosing gait pathologies and in the design of more agile robots.

1. Introduction

Locomotion is critical to survival and reproduction in most animals. A critical feature of successful locomotion is selection and maintenance of gait. While it has been shown that animals, including humans, choose gaits that appear to minimize energy consumption and injury risk (Hoyt et al., 1981; Farley et al., 1991), a large amount of variability exists in gait selection across animals (Hildebrand, 1989), and across conditions, such as treadmill (Blaszczyk et al., 1993) or rough terrain (Wilshin et al., 2017). Further, animals make fluid transitions between gaits; yet we have little understanding of how factors such as the mechanics of the different gaits influence these transitions (Ijspeert, 2007; Haynes, 2006).

Individuals often encounter perturbations during normal locomotion, from which they have to recover. Perturbations can also be used as a tool by an experimenter to elucidate mechanisms that are not observable in steady state conditions, and to better refine mathematical models, especially in the field of gait rehabilitation and robotics (Komura, et al., 2005; Schmidt, et al., 2005). Despite the utility of perturbation experiments both as a naturalistic stimulus and as a probe of control structure, ethical and experimental challenges have prevented full exploration of these in legged systems.

Biological studies utilizing perturbations of moving animals have lead to improvements in robots (Altendorfer et al., 2001; Haynes et al., 2009), given

insight into basic locomotor biomechanics (Jindrich and Full, 2002; Daley et al., 2006), and improved understanding of disease and injury in humans (Lamontagne et al., 2007; Protas et al., 2005). For instance, Gritsenko et al. (2001) studied the role of muscle activity and latency response of cats to unexpected perturbation before and after unilateral denervation of synergists. De Leon et al. (2000) also studied the relationship between the force control in flexor motor pools and adaptation to spinal cord injury in rats using gait perturbations. Similar studies have been carried out to analyze trained compensatory postural responses in older human adults during perturbed treadmill locomotion (Shapiro & Melzer, 2010). However, we have not found prior work that examines in detail the changes in gait by rodents in response to an unexpected mechanical perturbation. Characterizing such responses in rodents is important as they are becoming increasingly popular model systems in locomotion studies (Talpalar & Kiehn, 2010; Bellardita & Kiehn, 2015; Harris-Warrick, 2011), they provide a wide array of disease models (Rosenthal, 2007), and offer a wide range of genetic tools to manipulate aspects of both the neuro- and more general physiology (Lathe, 1996). Thus, here we examine the gait response of intact, freely running mice to a mechanical substrate perturbation.

Based on recent results in dogs walking on rough terrain (Wilshin, 2017), where perturbed gait at walking speeds was found to be restricted along the walk-trot line, it could be hypothesized that a similar anisotropy would exist at trot: e.g., that mice will exhibit perturbed gait around trot on the line between trot and walk.

However, the consideration for quasi-static stability that predicted the result in walking dogs is less likely to apply at the trotting speeds commonly used by rodents. Therefore it is unclear how to make a similar *a priori* prediction for the structure around trot without a model of dynamic stability that can be incorporated into our gait analysis framework. We therefore carried out the following exploratory study of mouse gait control about the trot.

2. Materials and Methods

A computer vision controlled treadmill system capable of applying rapid, precisely timed, and spatially confined mechanical perturbations to freely running mice was the central piece of apparatus (Fig. 1).

2.1. Materials

2.1.1. Animals

Eight adult female C57BL/6J mice were used in this study (<http://jaxmice.jax.org/strain/013636.html>). Animals were housed under a 12 : 12 h light-dark cycle in a temperature-controlled environment with food and water available *ad libitum*. Animal procedures were approved by the Temple University Institutional Animal Care and Use Committee ACUP #4675.

2.1.2. Treadmill-Camera System

We used a video-tracking, closed-loop treadmill system to control perturbation application and improve yield. The system uses employs a real-time feed of the position and speed of the mouse to adjust the belt speed (Spence et al., 2013). The system is built upon a Panlab Model Number LE8700 treadmill. Two cams, in the shape of $\frac{1}{2}$ of a disk, were machined and mounted on a shaft, running beneath the treadmill surface, under the belt. Slots cut in the belt support surface allowed these cams to push upward and deflect the surface. These cams produced small “earthquakes” (Fig. 1). To achieve fast motor response times, the motors and control system for the substrate deflection and the treadmill belt were essentially a two-legged version of the X-RHex robot (Haynes et al., 2012), where treadmill functionality replaced legged robot code.

The real-time feed was further used to trigger the mechanical perturbations, randomized between the left and right sides of the belt. We randomized the side of perturbation because in preliminary experiments we found that mice quickly learned which side of the treadmill contained the perturbation and would avoid it. This “behavioral triggering” based on the feed of animal position and speed can minimize the confounding effects due to variation in quantities such as speed, acceleration, and/or position relative to the earthquake. The perturbation was automatically triggered if the mice were running continuously for at least 0.75 sec, with a speed between 0.2 - 0.5 m/s (Video S1). An average-weight mouse of

30 g has a preferred speed of 0.46 m/s and trots in the range of 0.19–0.67 m/s (Spence et al., 2013; Herbin et al., 2004). A custom five camera high-speed video system was used to gather the kinematic data. For three of the mice an earlier version of the system consisting of two mirrors and two cameras, one for the real-time feed and the other for recording high-speed videos, was used, as described in Spence et al., 2013.

2.2 Experimental Design

2.2.1 Animal Training

All mice were trained daily (M-Th) for 2 weeks to run on the treadmill prior to collecting data. The first week of training session consisted of 10 minutes treadmill acclimation, with access to food rewards, before and after activating the treadmill, followed by 15 minutes of running on the treadmill. On the second week of trainings the automated perturbation was activated during their running trials.

2.2.2 Selection Criteria

We were interested in the trials that the animal was able to recover from the perturbation, and continue running. Therefore, we selected trials that the average speed for mice after the perturbation was at least 54% of the average speed

before. We analyzed a total of 42 trials, from 8 animals, ranging from 3 to 14 perturbation responses per animal. An example of an individual accepted trial is given in Fig. 2.

2.2.3 Kinematics

When a perturbation was triggered by the video tracking feed, high-speed videos were dumped from a ring-buffer in memory to disk, extending from 2 seconds before the perturbation to 2 seconds after. The paws were then tracked to produce their 2D locations. This was done either manually, using a custom MATLAB GUI, or with an automated rodent paw tracker (Haji Maghsoudi et al., 2016) that finds the centroid of the mouse body, and uses the body location in combination with color and temporal information across frames to determine the front and hind paw locations (Fig. 2A and 2B). The body centroid location was then subtracted from the paw position to produce paw positions relative to the body, and this time series was z-scored (which is the standard deviations from the mean) before being utilized to compute instantaneous phase. The z-scored, body coordinate system fore-aft paw positions of 3 mice for two strides before, during, and two strides after the perturbation are plotted in Fig. 2C. Black horizontal bars indicate the duration of the perturbation, which is approximately 200 milliseconds (ms).

2.2.4. Phaser

The 2D kinematic data obtained from tracking the paws were analyzed using a phase-based approach, as described in Spence et al. (2013) and Wilshin et al. (2017). This analysis assigns a three-dimensional value that defines paw relative phase characteristics and identifies where the gait lies with respect to “ideal” quadrupedal gaits.

With this approach each limb is considered as an oscillator and the limb phases are estimated for each time point. The limb phases, denoted $\theta_{FL}, \theta_{FR}, \theta_{HL}, \theta_{HR}$ are first estimated for each leg (Fig. 3A). This limb phase is an instantaneous estimate of where in a cycle the limb is, with 0 being the start of a cycle and 2π the end (Fig. 3B). The estimate of phase was made using the *Phaser* algorithm (Revzen 2008), which in turn relies on a Hilbert transformation and a Fourier series correction for systematics.

Gait is then characterized via phase differences between the continuous estimates of each limb’s phase. We denote individual leg phases as θ_i , and leg phase differences as ϕ_i . These three phase differences were calculated using Eq. (1) and estimate how far ahead or behind in a cycle one limb is relative to another:

$$\begin{aligned}\phi_1 &= \theta_{FL} - \theta_{HR} \\ \phi_2 &= \theta_{HR} - \theta_{HL} \\ \phi_3 &= \theta_{HL} - \theta_{FR}.\end{aligned}\tag{1}$$

To clarify how these phase differences represent gait, and how the ideal gaits are defined with this approach, we now compute them for trot and bound. Referring to the leg convention in Figure 3, we first choose a reference leg at phase 0: hind left. At trot, the fore-left limb is in phase with the hind-right, so $\phi_1 = \theta_{FL} - \theta_{HR} = 0$, and the fore-right is in phase with hind-left, $\phi_3 = \theta_{HL} - \theta_{FR} = 0$. Finally, hind-left and hind-right are out of phase by 180 degrees, so $\phi_2 = \theta_{HR} - \theta_{HL} = \pi$. Thus, the coordinates of trot with this convention are $(\phi_1, \phi_2, \phi_3) = (0, \pi, 0)$. Bound is computed similarly, with $(\theta_{FL}, \theta_{FR}, \theta_{HL}, \theta_{HR}) = (0, 0, \pi, \pi)$ such that $(\phi_1, \phi_2, \phi_3) = (\pi, 0, \pi)$. Fig. 4 illustrates this.

3. Results

The individual leg phases computed for one of the analyzed trials and corresponding three phase differences are shown in Fig. 5. The grey area indicates the perturbation. Transitory changes in phase advance can be seen in the individual limb phases in Fig. 5A. During the perturbation period specified in the gray box in Fig. 5B, the phase difference between FL-HR and HL-FR are shifting from 0 towards π and the phase difference between HR-HL is shifting from π towards 0. We note that this direction is towards bound, when starting at trot (trot is at $(0, \pi, 0)$ and bound is at $(\pi, 0, \pi)$); thus the direction from trot to bound is $(+1, -1, +1)$. Linear fits to the data in scatter plots of pairwise combinations of the leg phase differences (Figure 6) yield estimates for the slope

of the stride during the perturbation consistent with this direction (ϕ_2 vs ϕ_1 : -0.63 (-0.91 -0.36); ϕ_3 vs ϕ_1 : 0.32 (0.04 0.60257); ϕ_3 vs ϕ_2 : -0.70 (-0.86 -0.53); mean and confidence interval bounds; linear regression, n=42 strides from 8 mice).

To quantify the change in gait on a continuum we computed the projection of the observed gait onto the line (or circle, due to the topology of the space) between trot and bound. We refer to the value of this projection as λ , and note it is analogous to the one computed in Wilshin et al. (2017) that projects onto a line between walk and trot. We wish for this λ to treat changes in gait caused by any one leg to be considered movements of equal distance in gait space, but our leg phase difference transformation, without correction, would distort this. Thus we add an additional equation to those in Eq. 1 that will impose treating all limbs as equivalent. We refer to this fourth coordinate as the global phase, which is the average of the four phases with equal weight. This choice of global phase will disregard the overall, “mutual” phase advance of the four limbs, leaving only information about the relative phase difference, and is defined as:

$$\psi = \frac{1}{4} \sum_{\mu=0}^{\mu=FL,FR,HL,HR} \theta_{\mu} \quad (2)$$

We can now write a system of four equations that transform leg phases to leg phase differences in matrix form:

$$\begin{pmatrix} \phi_1 \\ \phi_2 \\ \phi_3 \\ \psi \end{pmatrix} = \begin{pmatrix} 1 & -1 & 0 & 0 \\ 0 & 1 & -1 & 0 \\ 0 & 0 & 1 & -1 \\ \frac{1}{4} & \frac{1}{4} & \frac{1}{4} & \frac{1}{4} \end{pmatrix} \begin{pmatrix} \theta_{FL} \\ \theta_{HR} \\ \theta_{HL} \\ \theta_{FR} \end{pmatrix} \quad (3)$$

Inverting this equation gives the transformation from leg phase differences to individual leg phases:

$$\begin{pmatrix} \theta_{FL} \\ \theta_{HR} \\ \theta_{HL} \\ \theta_{FR} \end{pmatrix} = \frac{1}{4} \begin{pmatrix} 3 & 2 & 1 & 4 \\ -1 & 2 & 1 & 4 \\ -1 & -2 & 1 & 4 \\ -1 & -2 & -3 & 4 \end{pmatrix} \begin{pmatrix} \phi_1 \\ \phi_2 \\ \phi_3 \\ \psi \end{pmatrix} = U\phi \quad (4)$$

We refer to the matrix above that transforms from ϕ to θ as U . We then use this transformation to define a metric that allows for computation of distance between points expressed in leg phase difference coordinates, but that will preserve equal contributions to distance from each of the four individual leg phases. For analogous examples in coordinate changes, see, e.g., Arfken (2005). We let G_{ij} be this induced metric derived from U :

$$G_{ij} = \sum_l \frac{\partial \theta_l}{\partial \phi_i} \frac{\partial \theta_l}{\partial \phi_j} = U^T U = \frac{1}{4} \begin{pmatrix} 3 & 2 & 1 & 0 \\ 2 & 4 & 2 & 0 \\ 1 & 2 & 3 & 0 \\ 0 & 0 & 0 & 16 \end{pmatrix} \quad (5)$$

To project points in ϕ space onto the line between trot and bound we calculate the distance between trot and desired point, using the metric to ensure the correct distance (starting in vector notation and then ending in matrix representation):

$$\begin{aligned} \lambda_{TB} &= ((\theta - \theta_T) \cdot n_{TB}) = ((U\phi - U\phi_T)^T U n_{TB}) = ((\phi - \phi_T)^T U^T U n_{TB}) \\ &= (\phi - \phi_T)^T G n_{TB} \end{aligned} \quad (6)$$

Where n_{TB} is a unit vector that has the same direction as the line from trot to bound ($\theta - \theta_T$) in the ϕ space and is calculated as follows:

$$\begin{aligned}
 n_{TB} &= \frac{\phi_B - \phi_T}{\|\phi_B - \phi_T\|} = \frac{(\pi, 0, \pi) - (0, \pi, 0)}{\|(\pi, 0, \pi) - (0, \pi, 0)\|} \\
 &= \frac{(\pi, -\pi, \pi)}{\sqrt{((U(\pi, -\pi, \pi))^T U(\pi, -\pi, \pi))}} = \frac{(\pi, -\pi, \pi)}{\sqrt{(\pi, -\pi, \pi)^T U^T U(\pi, -\pi, \pi)}} \\
 &= \frac{(\pi, -\pi, \pi)}{\sqrt{(\pi, -\pi, \pi)^T G(\pi, -\pi, \pi)}} = \frac{(1, -1, 1)}{\sqrt{1}} \tag{7}
 \end{aligned}$$

$$n_{TB} = \begin{pmatrix} 1 \\ -1 \\ 1 \\ 0 \end{pmatrix} \tag{8}$$

We note here that the leg phase differences formally have a fourth component, the global phase, as described above. We must compare all leg phase differences at the same global phase, but our choice of that global phase is arbitrary. As long as we compare leg phase differences at the same global phase, our comparisons are valid. By choosing it to be zero, the fourth component drops out of all calculations, and as such at times we simplify the notation by dropping the fourth component. If $\phi - \phi_T = \phi^r$,

$$\begin{aligned}
 \lambda_{TB} &= (\phi - \phi_T)^T G n_{TB} = (\phi_1^r \quad \phi_2^r \quad \phi_3^r \quad \psi^r) \frac{1}{4} \begin{pmatrix} 3 & 2 & 1 & 0 \\ 2 & 4 & 2 & 0 \\ 1 & 2 & 3 & 0 \\ 0 & 0 & 0 & 16 \end{pmatrix} \begin{pmatrix} 1 \\ -1 \\ 1 \\ 0 \end{pmatrix} \\
 &= \frac{1}{2} ((\phi_1 - \phi_1^T) + (\phi_3 - \phi_3^T)) = \frac{1}{2} (\phi_1 + \phi_3) \tag{9}
 \end{aligned}$$

λ thus indicates how far the gait is from the ideal trot or bound in each time point, noting that $\lambda_{TB} = 0$ when the gait is the ideal trot, and $\lambda_{TB} = \pm\pi$ for the ideal bound (Fig. 7).

The average λ over different trials across all mice is shown in Fig. 8A. There is a significant change in λ in both positive and negative direction after the perturbation was applied. On average, mice showed an increase in λ . The shift in λ in either direction corresponds to a change in gait that moves partially to bound from trot. Fig. 8B indicates the shift in λ towards bound before, during, and after the substrate perturbation. Using a mixed effects model, we assessed the relationship between λ and stride number relative to perturbation. The model contained a fixed effect for stride relative to perturbation, a mixed effect for mouse (N=8 mice; N=215 strides, $p_0=0.0002$ for the stride during the perturbation, $p_1=0.0027$ for the stride after the perturbation). The mixed effect model assumes that λ is normally distributed, which was verified through a Shapiro-Wilk test ($p=0.69$, $n=8$ mice) and visually confirmed with a q-q plot.

We analyzed the kinematic parameters speed, acceleration, and jerk (of the body) for the strides around the perturbation and explored whether they were correlated with changes in λ . We carried out a total of 15 hypothesis tests, comprised of three dependent variables, speed, acceleration, and jerk, against the five strides around the perturbation. The Bonferroni corrected p-value is 0.0033. Maximum absolute λ was not significantly dependent on speed of the

animal (linear mixed model; slope of λ against speed, with random effect for mouse; $p = 0.33$, $n = 8$ mice). However maximum positive jerk was correlated with maximum absolute λ for the stride during the perturbation (linear regression; $p = 0.00034$; $n=8$ mice; $R^2=0.56$; Fig. 9B). Other variables were statistically insignificant or had low R^2 values. Absolute values for λ were used because deviations away from zero in either direction correspond to changing gait toward bound, as described below. Fig. 9 shows jerk and λ time series aggregated for all trials across all mice. Jerk is seen to follow λ with a short delay (on the order of 100 ms). It may be that these changes in λ occur to bring the legs to a more effective phase relationship (e.g. closer to bound, hind legs and front legs in phase) for accelerative or decelerative behavior.

4. Discussion

Analyses of quadrupedal gait in biomechanics and neuroscience have typically considered the asymptotic, or steady state, behavior of gait, though gait transitions are certainly recognized as interesting and important phenomena (Kelso & Jeka, 1992; Kuo et al., 2005). Here we extend this to look at how gait evolves over shorter time scales, and develop tools that allow it to be placed in a continuum, or “gait space,” that includes the ideal gaits as fixed points. This aids examination of how gait recovers after perturbation, makes gait analysis more quantitative, and places gaits in an insightful context for biomechanical interpretation. We believe the temporal dynamics of gait control reveals

additional information that can't be seen without perturbation, and these mathematical tools capture that additional information parsimoniously.

Our data show that after mechanical perturbation mouse gait varies away from the trot but preferentially towards bound, may serve as a transitory gait before full stabilization is achieved and the mouse returns to a robust trot. We hypothesized that the transitions in gait that we observed may be related to the animal preparing to accelerate or decelerate rapidly (Walter et al., 2009; Lee et al., 1999). Quadrupeds accelerating from stand-still typically push simultaneously with their hind limbs for the first stride or two (Usherwood and Wilson, 2005), and thus having limbs in phase is likely to aid in acceleration, deceleration, or avoiding obstacles. Work in robotics has studied the stability of bounding quadrupeds (Iida and Pfeifer 2004; Poulakakis et al., 2006). Models of a robot were found to be relatively easily stabilized with a simple controller, or even without the need of any feedback control action. With certain bounding gaits, robots could rely on passive dynamic stability and/or operate, suggesting that bounding may be a relatively stable gait, especially when it comes to handling small perturbations (Iida et al., 2004; Poulakakis et al., 2006). To test this hypothesis in animals, future work could include electromyography during the perturbation (Akay et al., 2006) and look for anticipatory postural adjustments made by the animal in the face, to gain insight into whether these responses are feedforward versus feedback in nature.

Most animals exhibited positive λ value in response to perturbation; however two animals show negative λ on average (Fig. 8A). Here, we discuss in detail how the sign of λ is related to the phase of individual limbs. As the leg phase difference space is a three-dimensional torus (Fig. 6), negative values also correspond as shifts towards bound. One possible direction from trot to bound is [+1, -1, +1] in the three-dimensional phase difference coordinate system, which leads to positive values for λ . To transfer back to our θ coordinates, we can use:

$$\begin{pmatrix} \theta_{FL} \\ \theta_{HR} \\ \theta_{HL} \\ \theta_{FR} \end{pmatrix} = \frac{1}{4} \begin{pmatrix} 3 & 2 & 1 & 4 \\ -1 & 2 & 1 & 4 \\ -1 & -2 & 1 & 4 \\ -1 & -2 & -3 & 4 \end{pmatrix} \begin{pmatrix} \phi_1 \\ \phi_2 \\ \phi_3 \\ \psi \end{pmatrix}$$

This direction from trot to bound can be expressed as the vector:

$$n_{TB} = \begin{pmatrix} 1 \\ -1 \\ 1 \\ 0 \end{pmatrix}$$

Thus the change in the individual leg phases, n_θ , for the above direction is:

$$\frac{1}{4} \begin{pmatrix} 3 & 2 & 1 & 4 \\ -1 & 2 & 1 & 4 \\ -1 & -2 & 1 & 4 \\ -1 & -2 & -3 & 4 \end{pmatrix} \begin{pmatrix} 1 \\ -1 \\ 1 \\ 0 \end{pmatrix} = \begin{pmatrix} 0.5 \\ -0.5 \\ 0.5 \\ -0.5 \end{pmatrix} \quad (10)$$

This implies that for animals to move from trot to bound in the [+1, -1, +1,] direction in the phase difference coordinate system, they have to adjust their individual limbs in [+0.5, -0.5, +0.5, -0.5] direction. $|\theta_{HR}|$ and $|\theta_{FR}|$ phases should increase and $|\theta_{HL}|$ and $|\theta_{FL}|$ decrease. Thus the left limbs speed up and the

right limbs slow down for positive λ , and an example of a trial with positive λ is seen in Fig 10a. Another possible direction is [-1, +1, -1,] (Figure 7). In that case:

$$\frac{1}{4} \begin{pmatrix} 3 & 2 & 1 & 4 \\ -1 & 2 & 1 & 4 \\ -1 & -2 & 1 & 4 \\ -1 & -2 & -3 & 4 \end{pmatrix} \begin{pmatrix} 1 \\ -1 \\ 1 \\ 0 \end{pmatrix} = \begin{pmatrix} -0.5 \\ +0.5 \\ -0.5 \\ +0.5 \end{pmatrix} \quad (11)$$

Which means that the right limbs speed up and the left limbs slow down, as is seen in Fig. 10B.

It has been shown that there is a bistable region for trot and bound as a function of frequency (Danner et al., 2016; Fig 3a; Danner et al. 2017; Fig 5a). This could suggest that the structure of gait regulation around trot has a bias towards bound. Future work could use mathematical analyses or simulated perturbations at trot within the model that these authors have developed to see whether it shows a relaxed recovery from perturbations toward bound.

Bellardita & Kiehn (2015) reported that bounding results when certain spinal interneurons (the V0s) are genetically ablated. An interesting future direction would be to study the perturbation recovery of these mice to determine whether their gait regulation still lies on the trot to bound axis/circle.

Overall, our findings may aid in the neuromechanical study of animals by showing how subtle shifts in gait emerge at multiple levels of analysis. They may reflect the structure of neural circuits, be responses to a number of environmental cues, or be behavioral preparations for certain tasks or contexts. It may also

suggest directions for robotics applications, where a partial gait adaptation response to environmental uncertainty could better prepare robots to react to unexpected disturbances.

Acknowledgements

This material is based upon work supported by, or in part by, the U. S. Army Research Laboratory and the U. S. Army Research Office (Grant no: W911NF1410141), and the Shriners Hospitals for Children Research (Grant no: 85115). The authors thank all the members of academy and staff at Temple University, especially Matthew Short, for helping with collecting data, and Helen Freitas for her highly valued support.

Conflict of Interest Statement

We hereby declare that we have no financial or personal relationships with other people or organizations that could inappropriately influence (bias) our work.

References

- Akay, T., Acharya, H. J., Fouad, K., & Pearson, K. G. (2006). Behavioral and electromyographic characterization of mice lacking EphA4 receptors. *Journal of neurophysiology*, 96(2), 642-651.
- Altendorfer, R., Moore, N., Komsuoglu, H., Buehler, M., Brown, H. B., McMordie, D., ... & Koditschek, D. E. (2001). Rhex: A biologically inspired hexapod runner. *Autonomous Robots*, 11(3), 207-213.
- Arfken, G. B., Weber, H. J., & Harris, F. E. (1995). *Mathematical methods for physicists: a comprehensive guide*. Academic press.
- Bellardita, C., & Kiehn, O. (2015). Phenotypic characterization of speed-associated gait changes in mice reveals modular organization of locomotor networks. *Current Biology*, 25(11), 1426-1436.
- Blaszczyk, J., & Loeb, G. E. (1993). Why cats pace on the treadmill. *Physiology & behavior*, 53(3), 501-507.
- Daley, M. A., Usherwood, J. R., Felix, G., & Biewener, A. A. (2006). Running over rough terrain: guinea fowl maintain dynamic stability despite a large unexpected change in substrate height. *Journal of experimental biology*, 209(1), 171-187.
- Danner, S. M., Wilshin, S. D., Shevtsova, N. A., & Rybak, I. A. (2016). Central control of interlimb coordination and speed-dependent gait expression in quadrupeds. *The Journal of physiology*, 594(23), 6947-6967.
- Danner, S. M., Shevtsova, N. A., Frigon, A., & Rybak, I. A. (2017). Computational modeling of spinal circuits controlling limb coordination and gaits in quadrupeds. *Elife*, 6, e31050.
- De Leon, R. D., Timoszyk, W., London, N., Joynes, R. L., Roy, R. R., Reinkensmeyer, D. J., & Edgerton, V. R. (2000). Locomotor adaptations to robot-applied force fields in spinally transected rats. In *Soc. Neurosci. Abstr* (Vol. 26, p. 697).
- Farley, C. T., & Taylor, C. R. (1991). A mechanical trigger for the trot-gallop transition in horses. *Science*, 253(5017), 306-308.
- Gritsenko, V., Mushahwar, V., & Prochazka, A. (2001). Adaptive changes in locomotor control after partial denervation of triceps surae muscles in the cat. *The Journal of physiology*, 533(1), 299-311.
- Harris-Warrick, R. M. (2011). Neuromodulation and flexibility in central pattern generator networks. *Current opinion in neurobiology*, 21(5), 685-692.
- Haynes, G. C., & Rizzi, A. A. (2006, May). Gaits and gait transitions for legged robots. In *Robotics and Automation, 2006. ICRA 2006. Proceedings 2006 IEEE International Conference on* (pp. 1117-1122). IEEE.
- Haynes, G. C., Khripin, A., Lynch, G., Amory, J., Saunders, A., Rizzi, A. A., & Koditschek, D. E. (2009, May). Rapid pole climbing with a quadrupedal robot. In *Robotics and Automation, 2009. ICRA'09. IEEE International Conference on* (pp. 2767-2772). IEEE.
- Haynes, G. C., Pusey, J., Knopf, R., Johnson, A. M., & Koditschek, D. E. (2012, June). Laboratory on legs: an architecture for adjustable morphology with legged robots. In *Unmanned Systems Technology XIV* (Vol. 8387, p. 83870W). International Society for Optics and Photonics.

Herbin, M., Gasc, J. P., & Renous, S. (2004). Symmetrical and asymmetrical gaits in the mouse: patterns to increase velocity. *Journal of Comparative Physiology A*, 190(11), 895-906.

Hildebrand, M. (1989). The quadrupedal gaits of vertebrates. *BioScience*, 39(11), 766.

Hoyt, D. F., & Taylor, C. R. (1981). Gait and the energetics of locomotion in horses. *Nature*, 292(5820), 239.

Iida, F., & Pfeifer, R. (2004, March). Cheap rapid locomotion of a quadruped robot: Self-stabilization of bounding gait. In *Intelligent Autonomous Systems* (Vol. 8, pp. 642-649). IOS Press Amsterdam, The Netherlands.

Ijspeert, A. J., Crespi, A., Ryczko, D., & Cabelguen, J. M. (2007). From swimming to walking with a salamander robot driven by a spinal cord model. *science*, 315(5817), 1416-1420.

Jindrich, D. L., & Full, R. J. (2002). Dynamic stabilization of rapid hexapedal locomotion. *Journal of Experimental Biology*, 205(18), 2803-2823.

Kelso, J. A., & Jeka, J. J. (1992). Symmetry breaking dynamics of human multilimb coordination. *Journal of Experimental Psychology: Human Perception and Performance*, 18(3), 645.

Komura, T., Leung, H., Kudoh, S., & Kuffner, J. (2005, April). A feedback controller for biped humanoids that can counteract large perturbations during gait. In *Robotics and Automation, 2005. ICRA 2005. Proceedings of the 2005 IEEE International Conference on* (pp. 1989-1995). IEEE.

Kuo, A. D., Donelan, J. M., & Ruina, A. (2005). Energetic consequences of walking like an inverted pendulum: step-to-step transitions. *Exercise and sport sciences reviews*, 33(2), 88-97.

Lamontagne, A., Stephenson, J. L., & Fung, J. (2007). Physiological evaluation of gait disturbances post stroke. *Clinical Neurophysiology*, 118(4), 717-729.

Lathe, R. (1996). Mice, gene targeting and behaviour: more than just genetic background. *Trends in neurosciences*, 19(5), 183-186.

Lee, D. V., Bertram, J. E., & Todhunter, R. J. (1999). Acceleration and balance in trotting dogs. *Journal of Experimental Biology*, 202(24), 3565-3573.

Maghsoudi, O. H., Tabrizi, A. V., Robertson, B., Shamble, P., & Spence, A. (2016, December). A rodent paw tracker using support vector machine. In *Signal Processing in Medicine and Biology Symposium (SPMB), 2016 IEEE* (pp. 1-3). IEEE.

Poulakakis, I., Papadopoulos, E., & Buehler, M. (2006). On the stability of the passive dynamics of quadrupedal running with a bounding gait. *The International Journal of Robotics Research*, 25(7), 669-687.

Protas, E. J., Mitchell, K., Williams, A., Qureshy, H., Caroline, K., & Lai, E. C. (2005). Gait and step training to reduce falls in Parkinson's disease. *NeuroRehabilitation*, 20(3), 183-190.

Revzen, S., & Guckenheimer, J. M. (2008). Estimating the phase of synchronized oscillators. *Physical Review E*, 78(5), 051907.

Rosenthal, N., & Brown, S. (2007). The mouse ascending: perspectives for human-disease models. *Nature cell biology*, 9(9), 993.

Schmidt, H., Piorko, F., Bernhardt, R., Kruger, J., & Hesse, S. (2005, June). Synthesis of perturbations for gait rehabilitation robots. In *Rehabilitation Robotics, 2005. ICORR 2005. 9th International Conference on* (pp. 74-77). IEEE.

Shapiro, A., & Melzer, I. (2010). Balance perturbation system to improve balance compensatory responses during walking in old persons. *Journal of neuroengineering and rehabilitation*, 7(1), 32.

Spence, A. J., Nicholson-Thomas, G., & Lampe, R. (2013). Closing the loop in legged neuromechanics: an open-source computer vision controlled treadmill. *Journal of neuroscience methods*, 215(2), 164-169.

Talpalar, A. E., & Kiehn, O. (2010). Glutamatergic mechanisms for speed control and network operation in the rodent locomotor CPG. *Frontiers in neural circuits*, 4, 19.

Usherwood, J. R., & Wilson, A. M. (2005). Biomechanics: no force limit on greyhound sprint speed. *Nature*, 438(7069), 753.

Walter, R. M., & Carrier, D. R. (2009). Rapid acceleration in dogs: ground forces and body posture dynamics. *Journal of Experimental Biology*, 212(12), 1930-1939.

Wilshin, S., Reeve, M. A., Haynes, G. C., Revzen, S., Koditschek, D. E., & Spence, A. J. (2017). Longitudinal quasi-static stability predicts changes in dog gait on rough terrain. *Journal of Experimental Biology*, 220(10), 1864-1874.

Wilshin, S., Haynes, G. C., Porteous, J., Koditschek, D., Revzen, S., & Spence, A. J. (2017). Morphology and the gradient of a symmetric potential predict gait transitions of dogs. *Biological cybernetics*, 111(3-4), 269-277.

Fig. 1. (A) Intact, running mice before, and (B) after applying perturbation. (C) Rendering of the treadmill, including the two perturbation disks.

Fig. 2. Mouse paw kinematic data for input to the phase estimator. (A, B) Still frames from automatically recorded, 2048 × 700 pixel, 250 Hz video of a running mouse captured in two cameras. (C) Example filtered fore/aft paw positions for two strides before, during, and two strides after the perturbation, for three mice. Line color denotes paw. Positions are the horizontal pixel coordinate of the paw relative to the body centroid, and normalized by z-scoring. Black horizontal bars and red vertical lines indicate the perturbation duration and peak. Red arrows indicate the change in gait in all three mice after the perturbation was applied.

Fig. 3. (A) Limbs represented as oscillators, having instantaneous phase θ_i . The numbering convention of the limbs is shown. (B) A single limb phase estimated from the processed limb kinematics using the *Phaser* algorithm (Revzen, 2008). The blue line denotes the instantaneous phase of the leg estimated from the red line, which is the oscillatory kinematic input signal (the filtered fore-aft position of the paw). The maximum and minimum values of the red kinematic signal correspond to the extreme anterior and posterior extreme positions of the paw relative to the body. The phase signal wraps from 2π to 0 at a fixed phase of the cycle (close to where the paw position crosses zero going positive), which we use to define stride cycles, and corresponds to mid-swing.

Fig. 4. Footfall ordering and the corresponding leg phase difference coordinates for when the animal is (A) trotting, and (B) bounding.

Fig. 5. (A) Paw phases, (B) paw phase differences, and (C) Overlay of λ for one of the trials. The grey area indicates the perturbation duration. The phase differences in (B) are computed from individual phases in (A) using Eq. (1). As phase difference is a circular variable, it could be plotted modulo 2π centered at $y=0$, where it would overlap the blue ϕ_1 . Trot is recognized as $(0, \pi, 0)$ or $(0, \pi, 2\pi)$, as plotted. As bound is $(0, \pi, 0)$, transitory movement of the phase difference triple towards this point is seen during the perturbation (grey). The mean value of each time series was computed within each pair of vertical blue lines denoting stride boundaries, and that these averages were used in the mixed effects models and box plots in subsequent analyses.

Fig. 6. Two-dimensional scatter plots of the animals' gait characterized by the three leg phase differences: (A) ϕ_2 vs ϕ_1 , (B) ϕ_3 vs ϕ_1 , and (C) ϕ_3 vs ϕ_2 . Each point represents the average over a complete stride, and points for all eight mice are overlaid. The data presents the strides two before, one before, containing, one after, and two strides after the mechanical perturbation. The gait is closer to the ideal trot gait for strides two and one before the perturbation (indicated as

strides -2 and -1) showing the preferred gait of these animals. In the stride in which the substrate perturbation occurs (stride 0), and the stride following the perturbation (stride 1), the gait moves away from trot, preferentially along the line towards bound. The gait for two strides after the perturbation (stride 2) has returned to being centered about trot; suggesting that after two strides, on average, the animal has recovered from the perturbation and is trotting normally again. The black line in each figure indicates the fitted line for the data points of only the strides 0. The slopes for figures A, B, C are measured as -0.63, 0.32, -0.70 with p-values of 1.5761e-22, 0.00080475, 3.4578e-16 respectively. See also supplemental videos S2-S6 for the three-dimensional presentation of the data points.

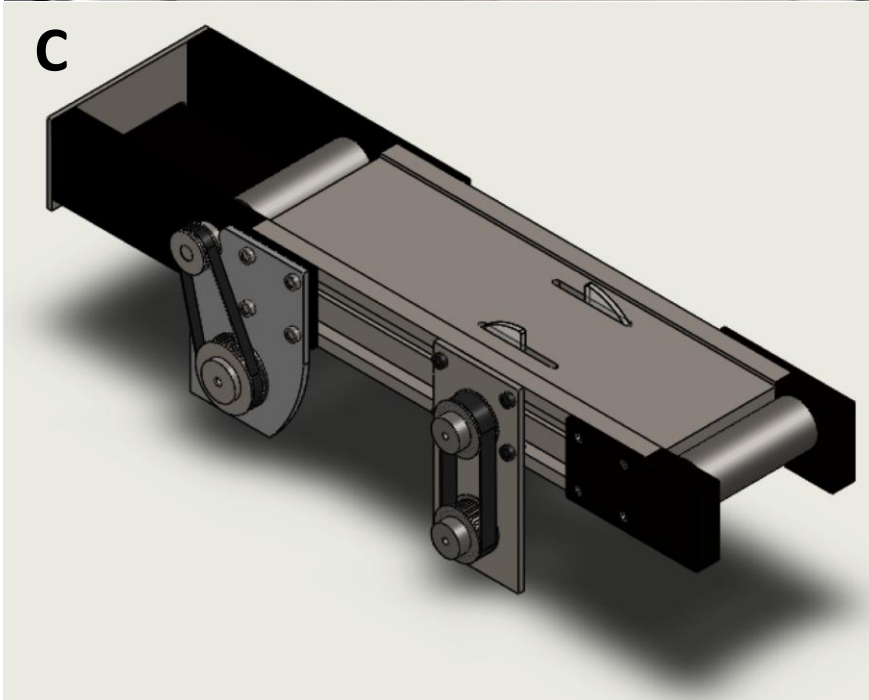
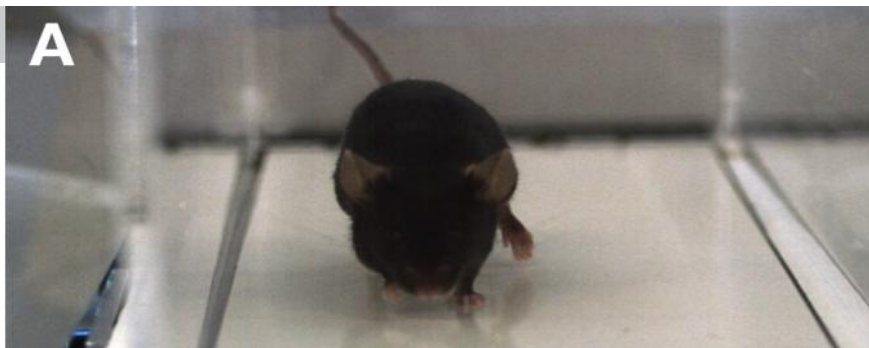
Fig. 7. Illustration of the projection onto the line between trot and bound. In order to quantify continuous shifts in gait between trot and bound, we compute the projection of the observed gait in the three-dimensional leg phase difference space (ϕ) onto a line between trot and bound (red line), as described in Eq. (9). We refer to this quantity as λ , which is normalized such that $\lambda=0$ at trot, and $\lambda=\pi$ at bound. We note that each leg phase difference variable is circular; and thus this space is a 3 dimensional torus. Thus, each face of the plot wraps at 0 and 2π . Thus, negative values of λ also correspond to movement toward bound, after wrapping around the torus. The difference between moving from trot to bound in positive versus negative directions corresponds to how the individual legs change their phase relationships: positive λ corresponds to speeding up the phase advance of the left side legs and slowing the advance of the right; negative λ the opposite (see Discussion for further details) (See also supplemental video S7).

Fig. 8. (A) Average λ as a function of time for each animal. The perturbation occurs at 200 ms. (B) Boxplot of λ over the stride where the perturbation occurred and two strides before and after. λ was significantly different in strides 0 and 1 (during the perturbation and one stride after the perturbation; linear mixed effects model; fixed effect for stride, random effect for mouse; $p_0=0.0002$, $p_1=0.0027$, $n=8$ mice). We note that (B) is not baselined to each individuals' first stride, in order to better illustrate the individual variation in λ , but that this choice masks the effect of the perturbation that the mixed effects model captures using a random effect for individual.

Fig. 9. (A) Aggregated, normalized time series for λ and body jerk. λ and jerk were aggregated first by averaging all trials within each mouse, and subsequently by averaging these averages across mice. The final time series were normalized to their maximum values. (B) A linear mixed effects model exhibited a statistically significant relationship between maximum λ and maximum jerk ($p = 0.00034$; $R^2 = 0.56$; $n=8$ mice). The dashed lines indicate the

90% predicted boundary. This correlation may indicate changes in gait that bring the front and hind legs in phase in preparation for acceleration or deceleration. Interestingly, these changes lie on a continuum, and can be transitory, which may have implications for the organization of neural or mechanical systems underlying gait.

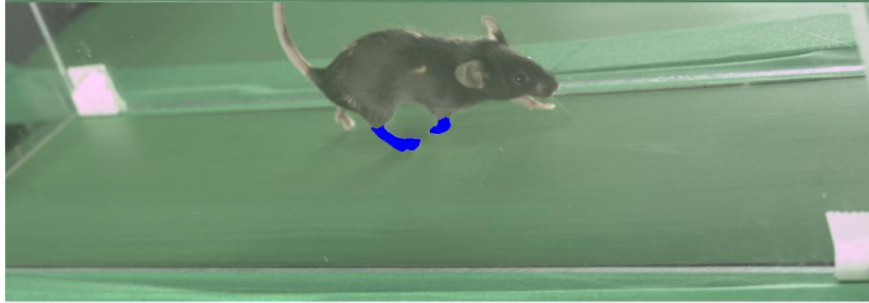
Fig. 10. Examples of individual perturbation trials illustrating transitory gait changes from trot towards bound in the positive (left column) and negative (right column) directions as defined by our parameter λ that captures the gait change along a line between trot and bound. Gait changes in the positive lambda direction correspond to an increase in the rate of phase advance of the left limbs and a concomitant slowing of phase advance of the right limbs. Negative changes in lambda correspond to the opposite changes. Rows depict lambda as (A, B) a function of time, (C, D) the leg phase differences, (E, F) individual leg phases detrended by the global phase, (G, H) the raw individual leg phases, and (I, J), a zoomed in time plot of the individual leg phases. A trial with a positive lambda excursion during the perturbation is shown in the left column (A, C, E, F, I), and negative lambda at right (B, D, F, H, J). Transitory changes in rate of phase advance of the left or right side pairs of legs can be seen in the raw leg phases (I, J). Whether animals' make their transitory gait changes with left or right side legs advancing in phase may depend on a "handedness" of mice, or potentially on small differences in their location relative to the perturbation.



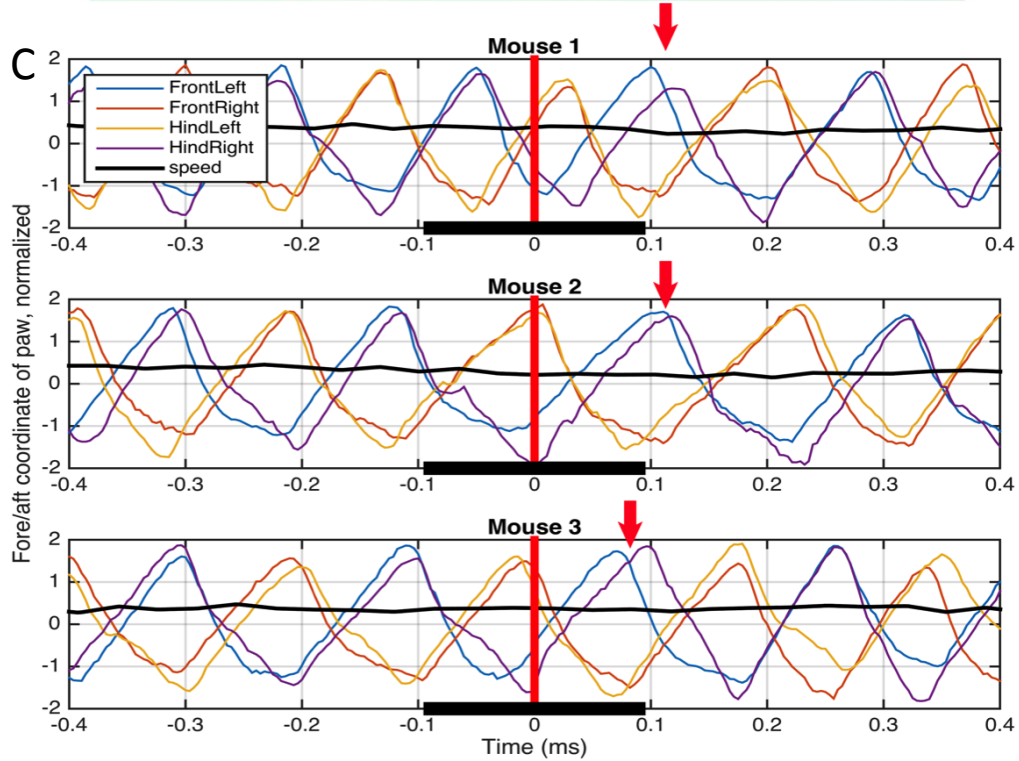
A



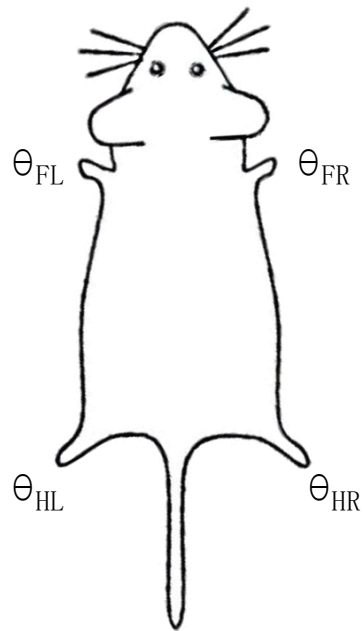
B



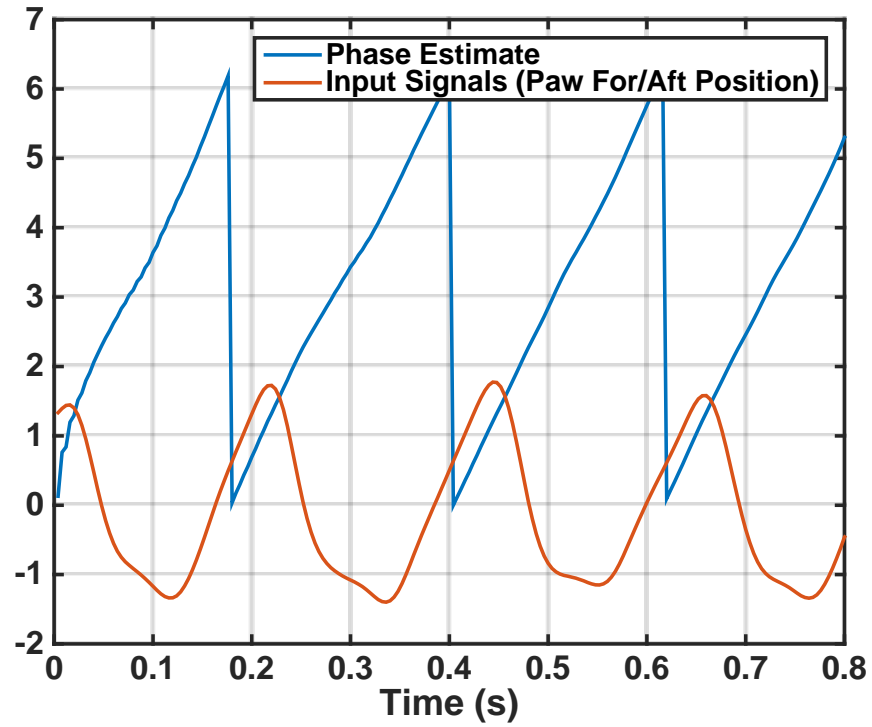
C



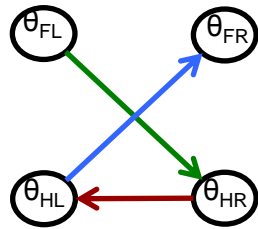
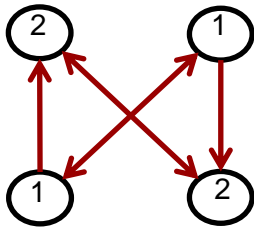
A



B

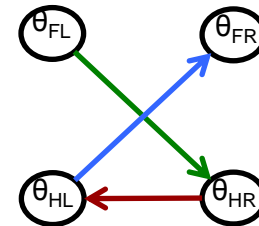
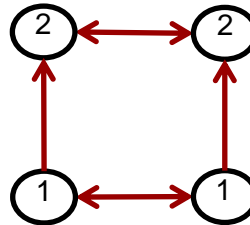


A. Trot

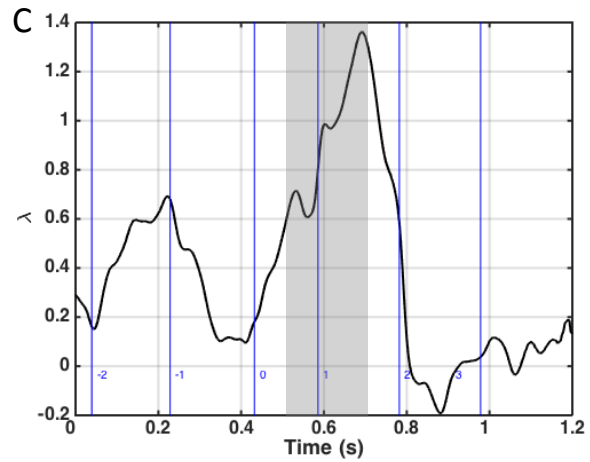
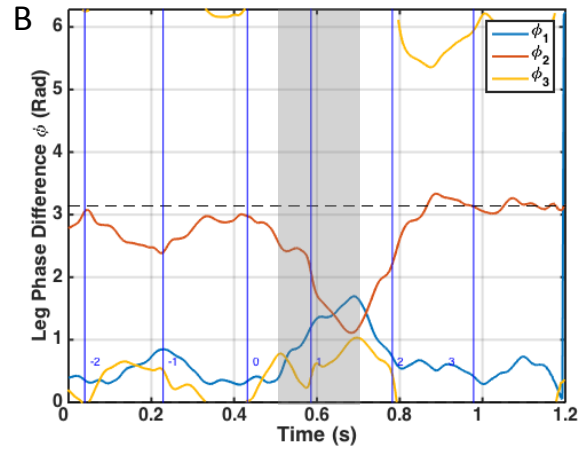
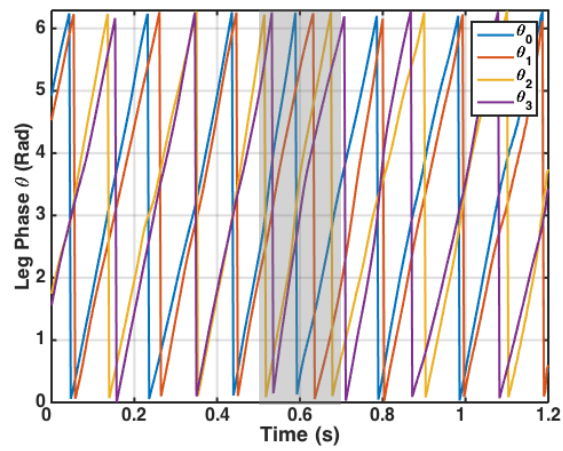


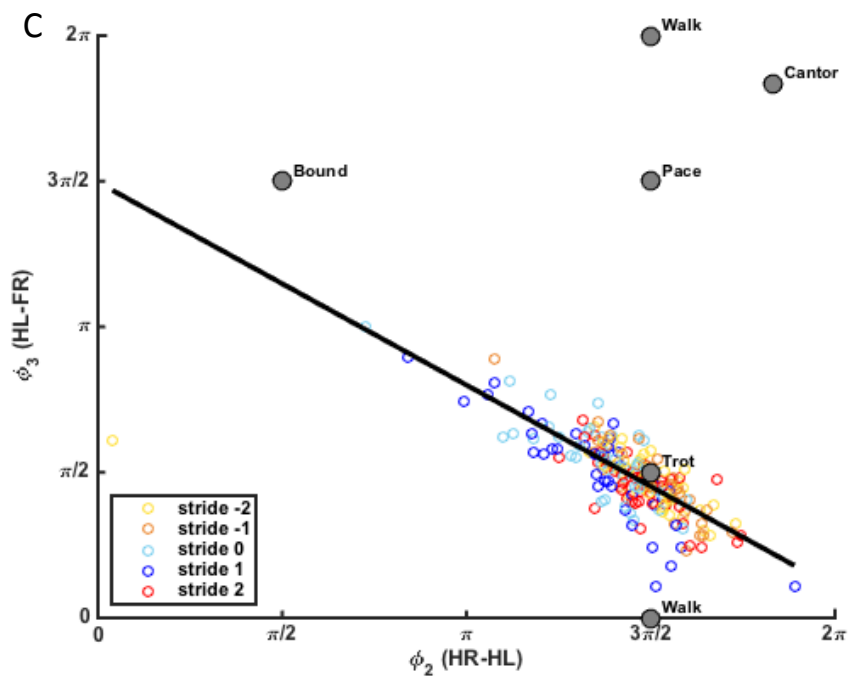
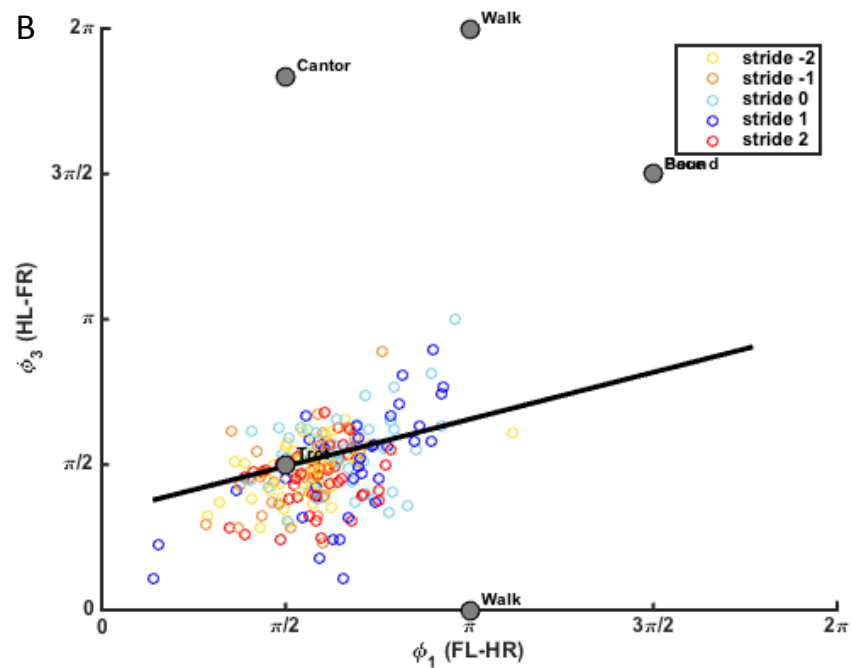
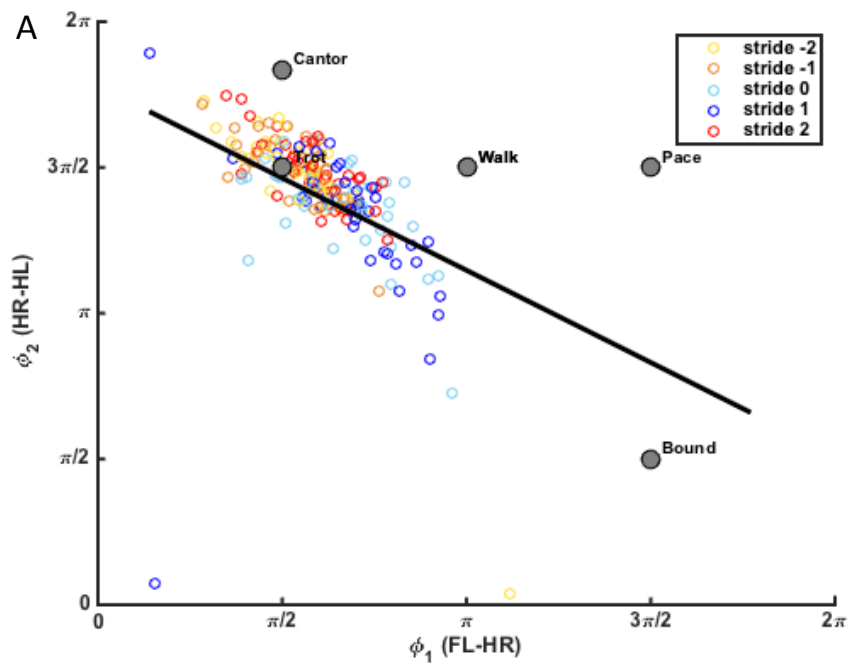
$$\begin{aligned}\phi_1 &= \theta_{FL} - \theta_{HR} = 0 \\ \phi_2 &= \theta_{HR} - \theta_{HL} = \pi \\ \phi_3 &= \theta_{HL} - \theta_{FR} = 0\end{aligned}$$

B. Bound



$$\begin{aligned}\phi_1 &= \theta_{FL} - \theta_{HR} = \pi \\ \phi_2 &= \theta_{HR} - \theta_{HL} = 0 \\ \phi_3 &= \theta_{HL} - \theta_{FR} = \pi\end{aligned}$$





Ideal Gait Locations and Trot-Bound Axis Projection λ

